

6-1-2004

Simulation of Hot Electron and Quantum Effects in AlGaIn/GaN Heterostructure Field Effect Transistors

N. Braga

R. Mickevicius

R. Gaska

H. Xu

M. S. Shur

See next page for additional authors

Follow this and additional works at: https://scholarcommons.sc.edu/elct_facpub



Part of the [Electrical and Electronics Commons](#), and the [Other Electrical and Computer Engineering Commons](#)

Publication Info

Published in *Journal of Applied Physics*, Volume 95, Issue 11, 2004, pages 6409-6413.

This Article is brought to you by the Electrical Engineering, Department of at Scholar Commons. It has been accepted for inclusion in Faculty Publications by an authorized administrator of Scholar Commons. For more information, please contact digres@mailbox.sc.edu.

Author(s)

N. Braga, R. Mickevicius, R. Gaska, H. Xu, M. S. Shur, M. Asif Khan, Grigory Simin, and J. Yang

Simulation of hot electron and quantum effects in AlGaIn/GaN heterostructure field effect transistors

N. Braga, R. Mickevicius, R. Gaska, X. Hu, M. S. Shur, M. Asif Khan, G. Simin, and J. Yang

Citation: *Journal of Applied Physics* **95**, 6409 (2004); doi: 10.1063/1.1719262

View online: <http://dx.doi.org/10.1063/1.1719262>

View Table of Contents: <http://scitation.aip.org/content/aip/journal/jap/95/11?ver=pdfcov>

Published by the [AIP Publishing](#)

Articles you may be interested in

[Contribution of alloy clustering to limiting the two-dimensional electron gas mobility in AlGaIn/GaN and InAlN/GaN heterostructures: Theory and experiment](#)

J. Appl. Phys. **116**, 133702 (2014); 10.1063/1.4896967

[Degradation and phase noise of InAlN/AlN/GaN heterojunction field effect transistors: Implications for hot electron/phonon effects](#)

Appl. Phys. Lett. **101**, 103502 (2012); 10.1063/1.4751037

[Quantum confinement effect on the effective mass in two-dimensional electron gas of AlGaIn/GaN heterostructures](#)

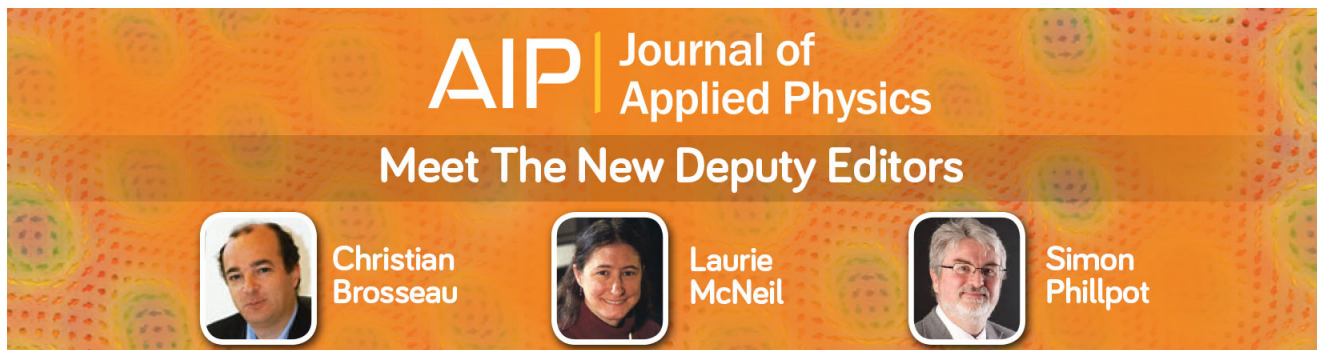
J. Appl. Phys. **105**, 073703 (2009); 10.1063/1.3100206

[A comparative study of effects of SiN_x deposition method on AlGaIn/GaN heterostructure field-effect transistors](#)

Appl. Phys. Lett. **94**, 053513 (2009); 10.1063/1.3079798



[Novel AlN/GaN insulated gate heterostructure field effect transistor with modulation doping and one-dimensional simulation of charge control](#)

J. Appl. Phys. **82**, 5843 (1997); 10.1063/1.366453



AIP | Journal of Applied Physics

Meet The New Deputy Editors

	Christian Brosseau		Laurie McNeil		Simon Phillpot
---	---------------------------	---	----------------------	---	-----------------------

Simulation of hot electron and quantum effects in AlGaIn/GaN heterostructure field effect transistors

N. Braga and R. Mickevicius

Integrated Systems Engineering Inc., San Jose, California 95113, USA

R. Gaska and X. Hu

Sensor Electronic Technology Inc., Columbia, South Carolina 29209, USA

M. S. Shur

Electrical, Computer, and Systems Engineering Department, Rensselaer Polytechnic Institute, Troy, New York 12180, USA

M. Asif Khan, G. Simin, and J. Yang

Department of Electrical Engineering, University of South Carolina, Columbia, South Carolina 29208, USA

(Received 3 November 2003; accepted 3 March 2004)

We report on simulations of electrical characteristics of AlGaIn/(InGaIn)/GaN heterostructure field effect transistors with quantum and hot electron effects taken into account. Polarization charges lead to quantum confinement of electrons in the channel and to the formation of two-dimensional electron gas. The electron quantization leads to the spread of the electron wave function into the barrier and bulk but does not have significant impact on dc electrical characteristics. Hot electrons play an important part in the charge transport by spilling over into the bulk GaN where they are captured by traps. This leads to negative differential conductivity, which is also observed experimentally. The simulation results are in good agreement with measured dc characteristics.

© 2004 American Institute of Physics. [DOI: 10.1063/1.1719262]

I. INTRODUCTION

In recent years, AlGaIn/GaN heterostructure field effect transistors (HFETs) and metal-oxide-semiconductor (MOS) HFETs have gained wide recognition as potential devices of choice for ultra-high-power microwave systems and power electronics. However, there are a number of issues, such as current collapse, trap memory effects, piezoelectric effects, and self-heating, where quantitative understanding is not yet achieved. This impedes widespread practical applications of III-nitride HFETs.

The usual approach employed to gain quantitative insight into the above mentioned phenomena is physics-based device simulation to complement experimental measurements.¹ However, physical models of III-nitride materials have not been well established. There are many discrepancies in the literature,² including recent dramatic revisions of the band gap parameter for InN.³ Moreover, mole fraction dependencies of many parameters remain unknown.

There have been a few recent publications dedicated to GaN HFET simulations.^{1,4} However, in all simulations reported, two important factors on the device characteristics have been neglected. The first such factor is the role of quantum effects such as the formation of two-dimensional (2D) electron gas in the channel of the HFET and electron tunneling through heterointerfaces. Second, hot electron effects have been ignored when employing only the drift-diffusion transport model for HFET simulations. Both effects may lead to electron spreading into the bulk GaN and into the barrier, and might have a significant impact on the device performance.

The goal of this paper is to understand the underlying physics of carrier kinetics in III-nitride heterostructures and to select or develop physical models suitable for predictive simulations of III-nitride devices. We will focus on the two issues ignored in previous simulations: quantum and hot electron effects.

II. DEVICE DESCRIPTION

Typically, the device epilayer structures are grown by low-pressure metal organic chemical vapor deposition on insulating 4H-SiC substrates or on sapphire. Alternative substrates include bulk GaN⁵ and bulk AlN.⁶ The structure studied in this paper was grown on 4H-SiC. As described, for example, by Khan *et al.*,⁷ the AlGaIn/GaN layers for this structure are deposited at 1000 °C and 76 Torr. A 100 nm AlN buffer layer is first grown at a temperature of 1000 °C, followed by a 2 μm insulating GaN layer. A thin (4–5 nm) In_{0.015}Ga_{0.985}N layer is then sandwiched between the insulating GaN and a 25 nm Al_{0.3}Ga_{0.7}N nonintentionally doped barrier layer. We also have a low-level flux of trimethylindium present during the growth of all the layers of the structure. The presence of the indium surfactant helps in improving the surface and interface roughness by incorporation of trace amounts of indium. The measured room temperature Hall mobility and sheet carrier concentration are 1100–1200 cm²/V-s and 8 to 9 × 10¹² cm⁻², respectively.

Transistor devices are fabricated using Ti(20nm)/Al(50nm)/Ti(20nm)/Au(150nm) for the source-drain ohmic contacts. The contacts are annealed at 850 °C for 1 min. in nitrogen ambient. A multiple He implant with energies of 10, 50, and 100 keV and a dose of (1–2) × 10¹⁵ cm⁻² is used

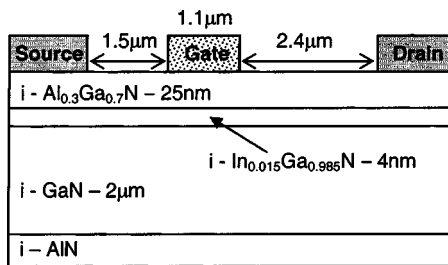


FIG. 1. Sketch of the HFET structure.

for device isolation. The gate deposition completes the fabrication process. Figure 1 shows a sketch of the fabricated structure.

III. SIMULATIONS

The simulations were performed for the long channel HFET fabricated as described in the preceding section. The simulation tool of choice was the multidimensional device simulator DESSIS from integrated Systems Engineering.⁸ Although DESSIS is capable of handling nonisothermal simulations, we assumed a fixed temperature of $T=300$ K in all simulations since self-heating effects go beyond the scope of this work and experimental I_D-V_{DS} curves (see Fig. 4) indicate that no significant self-heating occurs within the range of applied biases investigated in this work.

GaN and related compounds present several challenges to device simulators. First, there are significant polarization charges at heterointerfaces. AlGa_n, InGa_n, and GaN possess polarized wurtzite crystal structures, having dipoles across the crystal in the [0001] direction. In the absence of external fields, this macroscopic polarization includes spontaneous (pyroelectric), and strain induced (piezoelectric) contributions.⁹ The primary effect of polarization is an interface charge due to abrupt variations in the polarization at the AlGa_n/InGa_n heterointerface. Theoretical calculation of the total interface charge at a strained Al_{0.3}Ga_{0.7}N/In_{0.015}Ga_{0.985}N interface using average reported data on pyroelectric and piezoelectric components results in interface charges of around $(1.5-1.7) \times 10^{13} \text{ cm}^{-2}$.^{10,11} A partial strain relaxation might lead to a reduction of the polarization charges¹² and formation of significant amount of interface electron traps that partially neutralize the polarization charges. These effects combined should reduce the sheet charge density significantly. We adopted an effective interface charge density of $1.15 \times 10^{13} \text{ cm}^{-2}$ in all simulations. This, combined with adopted values for bulk trap concentrations discussed below, and the Schottky barrier height, allowed us to match experimentally observed values for the pinch-off voltage.

A Schottky barrier height of $\phi_B=1.55$ V was estimated based upon the experimental observation that the barrier for metal/AlGa_n contacts increases from that for metal/GaN contacts by approximately 0.02 V for every 1% increment in the Al mole fraction.¹³

Important model parameters for GaN, InN, and AlN, such as energy band structure, mobilities, and saturation velocities were based on the book by Levinshtein, Rumyantsev, and Shur² and a recent review of band parameters.³ Linear

TABLE I. Summary of parameter values at 300 K adopted in all simulations.

	GaN	InN	AlN
Dielectric constant	9.5	15.3	8.5
Energy gap (eV)	3.47	0.8	6.2
Electron Affinity (eV)	3.4	5.8	1.9
Electron mobility (cm ² /V-s)	1100	2400	300
Electron saturation velocity (cm/s)	1.2×10^7	2.6×10^7	1.5×10^7
Effective conduction band density of states (cm ⁻³)	2.65×10^{18}	1.3×10^{18}	4.1×10^{18}
Energy relaxation time (ps)	0.1	0.1	0.1

interpolations were adopted to compute parameter values as a function of mole fraction in AlGa_n and InGa_n. Table I summarizes important parameter values adopted in the simulations.

The only parameter whose value was significantly changed from the references was the GaN electron saturation velocity v_s . We had to reduce v_s by about 40% in order to fit experimentally observed values for the saturation current.

Hot electrons have been taken into account by employing a hydrodynamic (or energy balance) transport model.^{14,15} As a rule, long channel devices do not mandate the use of the hydrodynamic transport model to account for hot electrons. However, in GaN HFET, hot electrons play an important role in the vertical real space transfer and subsequent capture by bulk traps.

Due to the relatively immature state of III-nitride technology, these materials tend to exhibit a significant amount of structural defects, such as threading or misfit dislocations or carbon impurities, which translate into bulk traps.^{16,17} Traps are responsible for memory (hysteresis) effects and current collapse.¹⁸ We included only acceptor/electron bulk traps in our simulations since the primary quasistationary effect of interface/surface traps was accounted for by defining effective interface polarization charges. The density of acceptor type electron bulk traps in our simulations was $N_T=5 \times 10^{17} \text{ cm}^{-3}$, with a cross section of $\sigma_{Tn}=1 \times 10^{-15} \text{ cm}^{-2}$; we positioned these 1 eV above mid band gap. There are indications that multiple trap levels exist in III-Nitride materials.^{16,17} However, some trap parameters are still largely unknown. Therefore, we assumed just a single trap level and tuned trap parameter values to a reasonable fit of simulated IV curves with experimental data. We think that important trap-related electrical behavior was captured adequately in our simulations. Our test simulations indicate that multiple trap levels may lead to even better match between experiment and simulation with increasing degrees of freedom.

Because of polarization charges and a large conduction band offset, the electrons are subjected to quantum confinement at the AlGa_n/InGa_n interface (channel). A two-dimensional electron gas in the channel screens the polarization, as first predicted by Bykhovski *et al.*^{19,20} This screening is automatically taken into account in the simulations via self-consistent solution of transport and Poisson equations. The quantum effects due to electron confinement have been accounted for by the density gradient (DG) transport

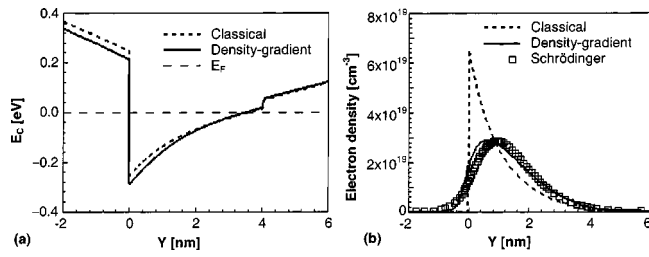


FIG. 2. Vertical cross section under the HFET gate with zero bias showing (a) the conduction band edge and Fermi level and (b) simulated electron density in the channel. Dashed lines show the result of classical simulations, and solid lines the corresponding results obtained with the density gradient model. For comparison the electron density from the Schrödinger approach is also shown with square markers.

model.²¹ The DG approach is a self-consistent way to account for quantum effects via quantum potential correction to the continuity equation.^{22,23} It has been shown in silicon devices that the DG model yields excellent quantitative agreement with self-consistent Poisson-Schrödinger solution under quasiequilibrium conditions.²⁴ However, unlike the Poisson-Schrödinger approach, the DG model is robust, fast, and can be applied to highly nonequilibrium situations. Moreover, the DG model can account for electron tunneling through the heterointerfaces in and from the channel.

IV. RESULTS AND DISCUSSION

Figure 2(a) shows the band structure along a vertical cross section under the gate at zero bias as predicted by a classical simulation and as predicted with the DG model. The conduction band edge predicted by both approaches coincides at the surface, 25 nm above the heterointerface. A very deep potential well is formed at the AlGaIn/InGaIn interface due to a large conduction band offset and polarization charges. This leads to quantum confinement of electrons in the channel and formation of 2D electron gas. The band bending seen in Fig. 2(a) is caused by the charging of deep bulk acceptor traps and, therefore, it flattens out as soon as the Fermi level rises above the trap energy level at ~ 0.7 eV below the conduction band edge in the bulk GaN. The corresponding distribution of electrons in the channel is shown in Fig. 2(b) under zero bias conditions. It is evident that the classical picture does not capture the quantum confinement of electrons. Both quantum approaches, namely, density gradient and Poisson-Schrödinger, are in good agreement with each other. Both quantum approaches and classical simulations yield similar values of the sheet electron density $n_s \approx 8 \times 10^{12} \text{ cm}^{-2}$, which is in good agreement with the experimentally measured value. However, the classical approach does not account for the significant penetration of the electron wave function into the wide band gap barrier layer and bulk GaN. Quantum calculations clearly show a significant penetration of the electron wave function from the 2D gas into AlGaIn and into three-dimensional states in GaN, thereby reducing the electron mobility.²⁵

Figure 3 compares the simulated and measured transfer characteristics ($I_D - V_G$). Simulations were performed with and without quantum corrections via DG. Because the sheet carrier densities are similar in the classical and quantum ap-

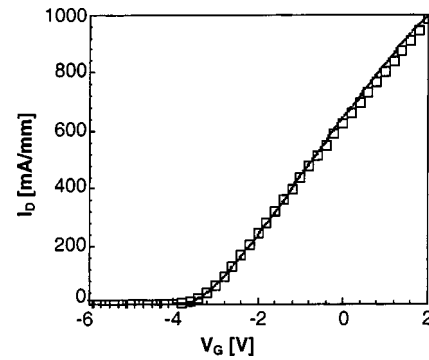


FIG. 3. Experimental (square markers) and simulated transfer characteristics ($I_D - V_G$) with quantum correction via DG (solid line). Drain voltage $V_D = 10$ V.

proaches, the transfer characteristics are not much affected by the quantum confinement. The simulations are in good agreement with the measurements.

Figure 4 shows the simulated and measured dc output characteristics ($I_D - V_D$) for V_G values varying from 0 to -4 V in 1 V steps. To reveal the role of hot electrons, we performed simulations within hydrodynamic (HD) and drift-diffusion (DD) transport models. In both, HD and DD, we included quantum effects via DG.

All experimental curves display small negative differential output conductance (NDC). At first glance, one might want to attribute the NDC to self-heating effects. However, careful examination of the experimental curves shows that the onset of negative output conductance occurs at $V_D - V_G \approx 4.6$ V for all the curves. As a result, the potential drop at the gate/drain edge for these bias points leads to similar electron heating, hence supporting an explanation based on electron energy rather than lattice temperature. Furthermore, the power dissipated in the device at these points varies from ~ 0.1 to ~ 3 W/mm for the curves corresponding to $V_G = -4$ V and $V_G = 0$ V, respectively. This depicts a 30 fold variation in dissipated power from which we can conclude that the NDC observed at low drain biases is not caused by self-heating.

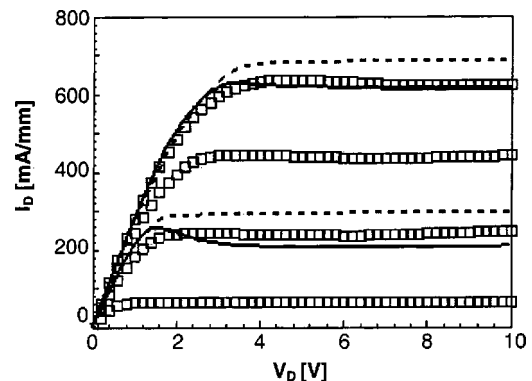


FIG. 4. Simulated and measured output characteristics ($I_D - V_D$). Experiment (square markers) for $V_G = 0, -1, -2,$ and -8 V, and simulation for $V_G = 0$ and -2 V, with hydrodynamic (solid lines) and drift-diffusion (dashed) approaches.

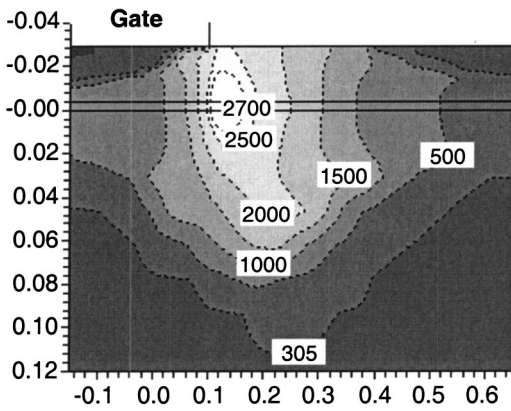


FIG. 5. Cross-section of the AlGaIn/InGaIn HFET around the gate edge near the drain showing an electron temperature contour map at $V_D=10$ V and $V_S=V_G=0$ V. Dimensions in μm .

According to our simulations, the NDC is compatible with the capture of hot electrons at bulk traps under sufficiently high drain bias conditions. Hydrodynamic transport simulations capture this effect while the simpler drift-diffusion approach yields completely flat saturation regions with no NDC. For large drain biases, electrons in the channel are significantly heated. Figure 5 shows a contour plot of the electron temperature distribution where a hot spot is observed in and around the channel on the drain side of the gate. The electrons in this location have enough energy to spread over the AlGaIn barrier and towards the GaN bulk.

Figure 6 compares simulated electron densities within drift-diffusion and hydrodynamic transport approaches. These snapshots were taken for a bias of $V_D=10$ V and $V_G=V_S=0$ V. We can clearly see that in drift-diffusion simulations electrons tend to be confined within the channel, while in hydrodynamic simulations the spreading of hot electrons towards the AlGaIn barrier and GaN substrate is evident.

At higher drain bias, the electrons become hotter; hence the wider flow spreading. An increase in drain bias results in more trap levels in the substrate being occupied with electrons. Figure 7 shows the distribution of captured electrons. This distribution follows the same pattern as the electron distribution except that it is significantly deeper. Moreover, there is occupation of a significant fraction of traps down to regions where the equilibrium electron concentration is only 10^7 cm^{-3} . This extra negative charge then lifts up the conduction band under the gate border near the drain, leading to

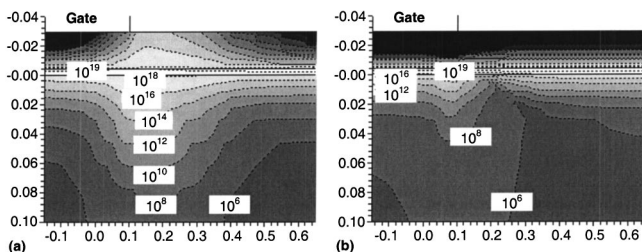


FIG. 6. Cross-section of the AlGaIn/InGaIn HFET with electron density contour maps comparing results predicted by (a) hydrodynamic and (b) simple drift-diffusion simulations. Dimensions in μm .

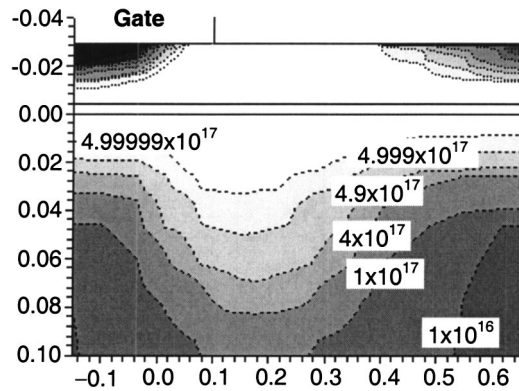


FIG. 7. Distribution of trapped electrons predicted by the hydrodynamic simulation at $V_D=10$ V and $V_S=V_G=0$ V. Dimensions in μm .

the formation of a potential barrier for the electron flow. That is consistent with the typical negative differential conductance observed in the experimental curves.

In order to visualize the formation of a potential barrier within the channel due to electron capture in bulk traps, we ran a simulation with an increased number of acceptor traps ($N_T=8 \times 10^{17} \text{ cm}^{-3}$) to exacerbate the NDC. Figure 8 shows cross sections of the HFET around the gate edge near the drain with conduction band edge E_C contour plots at $V_D=2.4$ V [Fig. 8(a)] and $V_D=6$ V [Fig. 8(b)] corresponding to drain biases at the current peak and valley, respectively, as pointed out in the $I_D - V_D$ curve in Fig. 8(c). Figure 8(d) shows a 3D surface plot corresponding to Fig. 8(b) for $V_D=6$ V where the presence of a conduction band barrier for electron flow is clearly visible in the gate edge region near the drain, hence giving rise to the NDC. The y scale (in the direction of device depth) in Fig. 8(d) has been considerably expanded so we can better visualize the rapid variations of the band just outside the channel towards the drain. The results shown in Fig. 8 support the model that relates current collapse to the trapping effects at gate edges.^{26,27}

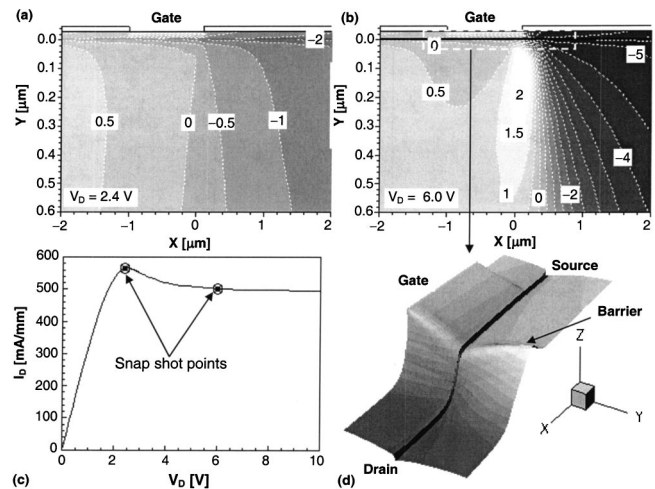


FIG. 8. Cross-sections of the HFET around the gate edge near the drain showing E_C contour plots at (a) $V_D=2.4$ V and (b) $V_D=6$ V corresponding to current peak and valley, respectively, as pointed out in the $I_D - V_D$ curve in (c). (d) shows a 3D surface plot with the presence of an E_C barrier for electron flow around the gate edge near the drain at $V_D=6$ V.

V. CONCLUSIONS

Polarization charges lead to quantum confinement of electrons in the channel of AlGaIn/GaN HFETs. To account for quantum effects we have employed a density gradient transport model implemented in the ISE device simulator DESSIS. Quantum calculations clearly show that a significant fraction of electrons in the 2D gas spreads into three-dimensional states in AlGaIn and GaN. This spreading does not affect dc electrical characteristics in a significant way but may become important in transient electron behavior. The simulation results are in good agreement with the experimental data.

Hot electrons play important part in the charge transport, even in long channel AlGaIn/GaN. They overcome potential barriers and spread to the barrier and bulk where they are captured by bulk traps. This leads to negative differential conductance in the output characteristics also observed experimentally.

The spreading of hot electrons to the barrier and bulk and their subsequent capture may have far more serious implications than minor negative differential conductance. Hot electron spreading strongly affects the breakdown voltage.²⁸ In the transient regime it may become the main contributor to the current collapse phenomenon. This effect remains outside the scope of this paper and will be addressed in the immediate future.

¹Y. Kawakami, N. Kuze, J.-P. Ao, and Y. Ohno, *IEICE Trans. Electron*, **E86-C**, 2039 (2003).

²*Properties of Advanced Semic. Mat.: GaN, AlN, InN, BN, and SiGe*, edited by M. E. Levinstein, S. Levinstein, S. L. Rumyantsev, and M. S. Shur (Wiley, New York, 2001).

³Davydov V. Yu, A. A. Klochkin, R. P. Seisyan, V. V. Emtsev, S. V. Ivanov, F. Bechstedt, J. Furthmuller, H. Harima, A. V. Mudryi, J. Aderhold, O. Semchinova, and J. Graul, *Phys. Status Solidi B* **229**, R1 (2002).

⁴G. Verzellesi, R. Pierobon, F. Rampazzo, G. Meneghesso, A. Chini, U. K. Mishra, C. Canali, and E. Zanoni, in *Proceedings of International Electron Devices Meeting*, (IEEE, Piscataway, NJ, 2002) p. 28.5.1.

⁵M. Asif Khan, J. W. Yang, W. Knap, E. Frayssinet, X. Hu, G. Simin, P. Prystawko, M. Leszczynski, I. Grzegory, S. Porowski, R. Gaska, M. S. Shur, B. Beaumont, M. Teisseire, and G. Neu, *Appl. Phys. Lett.* **76**, 3807 (2000).

⁶X. Hu, J. Deng, N. Pala, R. Gaska, M. S. Shur, C. Q. Chen, J. Yang, S.

Simin, A. Khan, C. Rojo, and L. Schowalter, *Appl. Phys. Lett.* **82**, 1299 (2003).

⁷M. Asif Khan, G. Simin, J. Yang, J. Zhang, A. Koudymov, M. S. Shur, R. Gaska, X. Hu, and A. Tarakji, *IEEE Trans. Microwave Theory Tech.* **51**, 624 (2003).

⁸DESSIS ISE TCAD Manual, Release 9.0 (ISE Integrated Systems Engineering AG, Zurich, 2002).

⁹F. Bernardini, V. Fiorentini, and D. Vanderbilt, *Phys. Rev. B* **56**, 10 024 (1997).

¹⁰R. Gaska, A. D. Bykhovski, and M. S. Shur, *Appl. Phys. Lett.* **73**, 3577 (1998).

¹¹O. Ambacher, J. Smart, J. R. Shealy, N. G. Weimann, K. Chu, M. Murphy, W. J. Schaff, L. F. Eastman, R. Dimitrov, L. Wittmer, M. Stutzmann, W. Rieger, and J. Hilsenbeck, *J. Appl. Phys.* **85**, 3222 (1999).

¹²R. Gaska, A. D. Bykhovski, and M. S. Shur, *Appl. Phys. Lett.* **73**, 3577 (1998).

¹³L. Yu, Q. J. Xing, D. Qiao, S. S. Lau, K. S. Boutros, and J. M. Redwing, *Appl. Phys. Lett.* **73**, 3917 (1998).

¹⁴R. Stratton, *Phys. Rev.* **126**, 2002 (1962).

¹⁵Y. Apanovich, E. Lyumkis, B. Polsky, A. Shur, and P. Blakey, *IEEE Trans. Comput.-Aided Des.* **13**, 702 (1994).

¹⁶X. H. Wu, L. M. Brown, D. Kapolnek, S. Keller, B. Keller, S. P. DenBaars, and J. S. Speck, *J. Appl. Phys.* **80**, 3228 (1996).

¹⁷P. B. Klein, S. C. Binari, K. Ikossi, A. E. Wickenden, D. D. Koleske, and R. L. Henry, *Appl. Phys. Lett.* **79**, 3527 (2001).

¹⁸M. A. Khan, M. S. Shur, Q. Chen, and J. N. Kuznia, *Electron. Lett.* **30**, 2175 (1994).

¹⁹A. Bykhovski, B. Gelmont, and M. S. Shur, *J. Appl. Phys.* **78**, 3691 (1995).

²⁰A. Bykhovski, B. Gelmont, and M. S. Shur, *Appl. Phys. Lett.* **63**, 2243 (1993).

²¹M. G. Ancona and H. F. Tiersten, *Phys. Rev. B* **35**, 7959 (1987).

²²D. K. Ferry and J.-R. Zhou, *Phys. Rev. B* **48**, 7944 (1993).

²³A. Wettstein, Ph.D. Thesis, ETH Zurich 2000, Hartung-Gorre, Konstanz, 2000.

²⁴E. Lyumkis, R. Mickevicius, O. Penzin, B. Polsky, K. El Sayed, A. Wettstein, and W. Fichtner, in *Proceedings of International Conference Simulations of Semiconductor Processes and Devices*, Kobe, Japan, 2002 (Business Center for Academic Societies, Japan, 2002) pp. 271–274.

²⁵E. Borovitskaya, W. Knap, M. Shur, R. Gaska, E. Frayssinet, P. Lorenzini, N. Grandjen, B. Beaumont, J. Massies, C. Skierbiszewski, P. Prystawko, M. Leszczynski, I. Grzegory, and S. Porowski, in *Proceeding of Material Research Society Symposium* **639**, G7.5, edited by G. Wetzel, M. Shur, U. K. Mishra, B. Gil, and K. Kishino (MRS, Warrendale, PA, 2001).

²⁶G. Simin, A. Koudymov, A. Tarakji, X. Hu, J. Yang, M. Asif Khan, M. S. Shur, and R. Gaska, *Appl. Phys. Lett.* **79**, 2651 (2001).

²⁷A. Koudymov, G. Simin, M. Asif Khan, A. Tarakji, M. Shur, and R. Gaska, *Electron Dev. Lett.* **24**, 680 (2003).

²⁸M. Dyakonov and M. S. Shur, *J. Appl. Phys.* **84**, 3726 (1998).